Bioactive Materials 6 (2021) 3194–3206

Contents lists available at ScienceDirect

Bioactive Materials

journal homepage: www.sciencedirect.com/journal/bioactive-materials

Ion therapy of pulmonary fibrosis by inhalation of ionic solution derived from silicate bioceramics

Tao Chen [a,1], Zhaowenbin Zhang [b,c,1], Dong Weng [a,1], LiQin Lu [a,1], XiaoYa Wang [b], Min Xing [b], Hui Qiu [a], MengMeng Zhao [a], Li Shen [a], Ying Zhou [a], Jiang Chang [b,**], Hui-Ping Li [a,*]

[a] Department of Respiratory Medicine, Shanghai Pulmonary Hospital, Tongji University, School of Medicine, Shanghai, China
[b] Shanghai Institute of Ceramics, Chinese Academy of Sciences, 1295 Dingxi Road, Shanghai, 200050, China
[c] Center of Materials Science and Optoelectronics Engineering, University of Chinese Academy of Sciences, 19 Yuquan Road, Beijing, 100049, People's Republic of China

ARTICLE INFO

Keywords:
Silicate bioceramics
Lung fibrosis
Alveolar epithelial cells II
Macrophages

ABSTRACT

Pulmonary fibrosis (PF) is a chronic and progressively fatal disease, but clinically available therapeutic drugs are limited due to efficacy and side effects. The possible mechanism of pulmonary fibrosis includes the damage of alveolar epithelial cells II (AEC2), and activation of immune cells such as macrophages. The ions released from bioceramics have shown the activity in stimulating soft tissue derived cells such as fibroblasts, endothelia cells and epithelia cells, and regulating macrophage polarization. Therefore, this study proposes an "ion therapy" approach based on the active ions of bioceramic materials, and investigates the therapeutic effect of bioactive ions derived from calcium silicate (CS) bioceramics on mouse models of pulmonary fibrosis. We demonstrate that silicate ions significantly reduce pulmonary fibrosis by simultaneously regulating the functions of AEC2 and macrophages. This result suggests potential clinical applications of ion therapy for lung fibrosis.

1. Introduction

Pulmonary fibrosis is a common feature of various lung diseases in advanced stage, which seriously affects the quality of life and prognosis of patients. The widely accepted hypothesis of the mechanism of pulmonary fibrosis is the damage of alveolar epithelial cells II (AEC2), and activation of immune cells such as macrophages, which leads to the up-regulation of inflammatory factors such as TGF-β that promote pulmonary fibrosis [1]. In addition, the cell viability of fibroblasts is also activated, which ultimately results elevated collagen deposition in the lung tissue [2]. Recently, in the COVID-19 pandemic pathophysiological changes of the lungs of COVID-19 patients are observed [3], which are consistent with the pre-pulmonary fibrosis reaction. It has also been observed from mouse animal models [4] that SARS-CoV-2 virus may infect AEC2, cause alveolar epithelial damage, and then activate macrophages to secrete various inflammatory factors, promote acute inflammation, and inhibit viral infection. If the inflammatory response cannot be controlled, it may develop into pulmonary fibrosis. Relevant clinical studies have shown that nearly 50% of COVID-19 patients will remain pulmonary fibrosis after being cured, and this mainly occurs in elderly patients with severe pneumonia [5]. Clinically, pirfenidone and nintedanib are currently available drugs for treatment of pulmonary fibrosis, which have limited efficacy and potential side effects [6–9]. For end-stage patients, lung transplantation is the only option, but its wide application is limited due to the lack of donor organs, immune rejection, and secondary infections after transplantation [10,11].

Under normal physiological conditions, AEC2 can proliferate and differentiate into alveolar epithelial cells I (AEC1) to repair damaged alveolar epithelium. In fibrotic lung tissue, the ability of AEC2 to proliferate is abnormal and large number of AEC2 cells reveal pro-fibrotic phenotype. The Wnt/b-catenin and Sonic-hedgehog pathways are activated to secrete a variety of growth factors and cytokines such as TGF-β and PDGF that promote fibrosis [12]. These biologically active substances can drive, recruit, and activate myofibroblasts, which then secret

Peer review under responsibility of KeAi Communications Co., Ltd.
* Corresponding author. Department of Respiratory Medicine, Shanghai Pulmonary Hospital, Tongji University, School of Medicine, 507 Zheng Min Road, Shanghai, 200433, China.
** Co-corresponding author. Shanghai Institute of Ceramics Chinese Academy of Sciences 1295 Dingxi Road, Shanghai, 200050, PR China.
E-mail addresses: jchang@mail.sic.ac.cn (J. Chang), liw2013@126.com (H.-P. Li).
[1] Contributed equally to this work.

https://doi.org/10.1016/j.bioactmat.2021.02.013
Received 15 December 2020; Received in revised form 9 February 2021; Accepted 13 February 2021

large amount of abnormal extracellular matrix (ECM) components to affect the normal alveolar structure and lead to pulmonary fibrosis. Therefore, after lung injury, how to regulate lung tissue-related cells (including AEC2 cells, fibroblasts, and bronchial epithelial cells), maintain their normal phenotype and function, and repair tissues at the injured site is a key point in the treatment of lung fibrosis.

In addition, alveolar macrophages are the first responsive cells of defense system responding to various stimuli during lung injury, and they are highly heterogeneous and plastic. In lung fibrotic tissue, after alveolar epithelial injury, the uncontrolled immune response will over-activate macrophages to express scavenger receptors and pro-fibrosis molecules, and AEC2 is activated to become a pro-fibrotic phenotype by some inflammatory factors including TGF-β, TNFα and IL-6 through paracrine mechanisms. This will also directly act on fibroblasts and promote the accumulation of ECM to form fibrosis [13]. Therefore, macrophage regulation is another key issue in the treatment of pulmonary fibrosis.

Silicate bioceramics such as calcium silicate (CS) are a kind of bioactive materials which release calcium (Ca^{2+}) and silicate ($4*10^3$) ions in body fluid, and its biological activity mainly attributes to the SiO_3^{2-} [14,15] ions, which do not show any toxicity effect in the body [16]. Studies have demonstrated that CS not only has activity to enhance hard tissue regeneration such as bone and tooth tissue [17,18], but also effective in stimulating soft tissue regeneration including the gastrointestinal tract, blood vessels, skin, and myocardium [19,20] by regulating stem cells [14] and tissue specific cells such as fibroblasts, skin epidermal cells [21], endothelia cells [22], cardiomyocytes [19,23]. A previous study has shown that Si-based biomaterial scaffolds can promote the adhesion and cell viability of AEC2 [24]. In addition to regulating stem proliferation, differentiation and cell viability of tissue-specific cells, recent studies have also revealed that silicate biomaterials can regulate macrophage polarization and inhibit expression of inflammatory factors (TNF-α, IL-1β and IL-10) by releasing active ions [25] for enhanced wound healing [26,27].

Considering the possible regulatory effects of SiO_3^{2-} on AECs, fibroblasts, epithelia cells and macrophages, which are critical cells involved in lung tissue fibrosis process, we assume that SiO_3^{2-} may also have the activity to inhibit fibrosis by affecting cellular activity of these cells. In this study, we investigated the interventional effects of CS-derived ionic solutions on pulmonary fibrosis using a pulmonary fibrosis mouse model (Fig. 1A), and the related mechanism of the effect of bioactive ions on pulmonary fibrosis was explored by studying the regulation of cell viability, migration, and apoptosis of three types of lung tissue cells, and the regulatory effect of ionic solution on macrophages.

2. Experimental section

2.1. Preparation of calcium silicate (CS) ionic solution

CS powder was prepared by chemical co-precipitation method [28], and the CS ionic solution was obtained according to previous published methods [29]. Briefly, 1 g of calcium silicate powder was added into 5 mL DMEM culture medium (for cell culture experiments) or PBS buffer saline (for animal experiments). Then, it was shaken in a shaker for 24 h at 37 °C at 120 rpm/min. The supernatant was collected by centrifugation at 4000 rpm/5 min and filtered through a 0.22 μm filter membrane to obtain CS ionic solution for further use. The ion concentration of the ionic solutions was measured by ICP-AES (Thermo Fisher X Series 2, USA).

2.2. Animal model establishment and CS intervention

A total of 105 SPF male C57BL/6 mice (Shanghai SLAC Laboratory Animal Co., Ltd) were used in this experiment (mouse age: 8 weeks old and average weight: 20–22 g). The specific groups of the experiment are as follows. (1) Normal control group: PBS + PBS, n = 10. (2) 1/8CS control group: PBS+1/8CS, n = 10. (3) CS control group: PBS + CS, n = 10. (4) Bleomycin model: BLM + PBS, n = 26. (5) 1/8CS intervention group: BLM+1/8CS, n = 23. (6) CS intervention group after BLM modeling: BLM + CS, n = 26. All animal experiments were approved by the Laboratory Animal Center of Tongji University (No. K17-016). In this study, bleomycin was used to induce pulmonary fibrosis. BLM (Dalian Meilun Biotech Co) is administered intratracheally at a dose of 3.5U/Kg, 40 μl/mouse. The BLM-induced pulmonary fibrosis model is dominated by acute inflammation from day 0 to day 7, and the fibrosis stage is from day 7 to day 21 [30,31]. Our hypothesis is that CS solution has inhibition effect on early acute inflammation, which may result in inhibition of pulmonary fibrosis. Therefore, the CS solution started to be applied 2 h after the BLM model was made at day 0. The CS solution started to be used 2 h after the BLM model was made. Two concentrations of CS ionic solutions were used. One is the 1/8 dilution due to its high bioactivity in stimulating epithelial cell proliferation observed in cell culture experiment. The other is the original CS extracts because it showed bioactivity in reducing myocardial fibrosis in our previous in vivo study [19,32].

The intervention design is shown in Fig. S1A and was performed by injecting 40 mL CS or 1/8CS solution through the oropharynx on the day of BLM modeling (D0), and injection of PBS was the control. Then, the injection was repeated every other day until the end of the experiment.

The alveolar lavage fluid (BALF) was collected on the 7th day (D7) and the 21st day (D21), and centrifuged at 1500r/min for 5min. Then, the supernatant was collected and stored at −80 °C for further use. The lung was also collected, the left lung and part of the right lung cryopreserved at −80 °C, and the remaining right lung was fixed with the tissue fixative (Wuhan Goodbio technology CO, LTD) for H&E and Masson staining.

2.3. Determination of mouse survival rate

In order to measure the mouse survival rate, the BLM modeling and CS intervention were conducted as described above with modification as shown in Fig. S1B), in which the CS intervention (CS and 1/8CS injection) only performed until day 6, and then the mice were kept until day 49. Then, the death of each group of mice in this time period was recorded, and the survival rate of mice was calculated.

2.4. Lung pathology

After 24 h fixation, the lung tissue was embedded in paraffin and sectioned followed by H&E and Masson staining. Then, the stained sections were scanned using a Leica Pathology Section Scanner (LEICA SCN400). H&E stained pathological sections were scored according to the ALI scoring standard reported by Mikawa et al. [33], and Masson staining was scored according to the pulmonary fibrosis scoring standard proposed by Hubner et al. [34] by two experienced pathologists independently to obtain average scores.

2.5. Determination of hydroxyproline in lung tissue

The analysis was performed with a piece of wet fresh lung tissue (30–60 mg) using an alkaline hydrolysis hydroxyproline kit (Nanjing Jiancheng Institute of Bioengineering, Nanjing) following the manufacture's instruction. The accurate weight of the tissue was record, the absorbance value at 550 nm was recorded, and the hydroxyproline content of lung tissue was calculated using the formula in the instruction manual. Specific steps are as follows:

The lung tissue was weighed and put into a test tube. The hydrolysis solution (1 mL) was added to the test tube and mixed well. Then, it is hydrolyzed in a boiling water bath for 20 min (mixing every 10 min of hydrolysis, the purpose is to make the hydrolysis more fully). The pH value is adjusted to around 6.0–6.8. Subsequently, an appropriate amount of activated carbon was added to the diluted hydrolysis solution and mixed. The sample was centrifuged for 10 min (3500 rpm). The

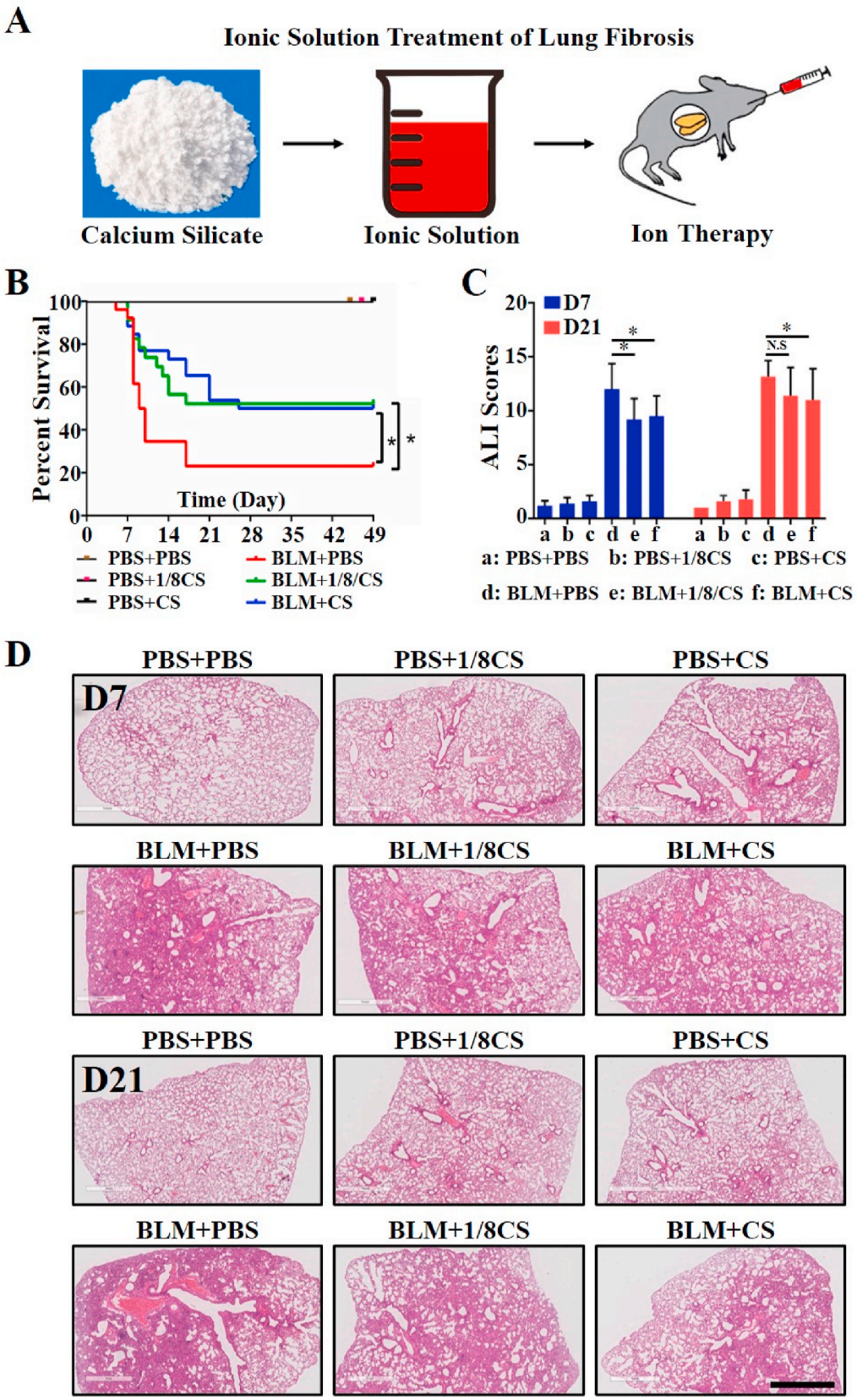

Fig. 1. The therapeutic effect of CS or 1/8CS ionic solution on BLM-induced lung fibrosis in mice. (A) Treatment of lung fibrosis with ionic solution derived from silicate bioceramics. (B) The mortality of mice within 49 days after BLM modeling. (C) ALI score results of mice in each group on D7 and D21. (D) H&E staining results of mouse lung tissue sections on D7 and D21 (Scale = 1 mm). (n = 5, *P < 0.05).

supernatant (1 mL) was taken out and the detection reagent was added. Then, the sample was bathed in water for 15 min (60 °C). And it was centrifuged for 10 min (3500 rpm). The absorbance of the supernatant after centrifugation was tested (550 nm).

2.6. Flow cytometry in bronchoalveolar lavage fluid (BALF)

After BALF centrifugation, the cells were collected, and the total number of cells was counted by Coomassie brilliant blue staining. Then, the cells were resuspended in FACS solution and divided into three parts. The staining was performed with the following antibodies such as anti-mouse CD11b-FITC, F4/80-APC, and Gr-1-PE; anti-mouse CD3-PE, CD4-FITC, and CD8-APC; and anti-CD4-FITC and CD25-PE (eBioscience, ThermoFisher, USA). After fixation and membrane rupture, cells were stained intracellularly with mouse FOX-P3-APC, and the fluorescence signals of the stained cells were measured by flow cytometry (CytoFLEX cytometer, Beckman-Coulter, USA). The specific parameters of the cell culture experiment are shown in Table S2.

2.7. Cell culture experiments

Considering that the involvement of a variety of lung-related tissue cells in lung fibrosis, alveolar epithelial cells II (A549), fibroblasts (MRC-5), bronchial epithelial cells (Beas-2B) and mouse macrophages (RAW.264.7) were used to study the regulatory effects of CS ionic solution. All cells were obtained from FuDan IBS Cell Center (Shanghai, China).

2.7.1. Effects of CS ionic solutions of different dilutions on the cell viability of A549, Beas-2B and MRC-5

CellTiter 96® A Queous One Solution Cell Proliferation Assay (MTS) (Promega Corporation, Madison, WI, USA) was used to detect cell viability. A549 ($4*10^3$/well), Beas-2B ($4*10^3$/well), and MRC-5 ($1*10^4$/well) were seeded in 96-well plates, where A549 and MRC-5 were cultured in DMEM+10%FBS+1%P/S while Beas-2B was cultured in DMEM+5%FBS+1%P/S. After 24 h, the culture medium was removed and replaced with the diluted CS ionic solution (The dilution concentrations are 1/2, 1/4, 1/8, 1/16, 1/32, 1/64 and 1/128 respectively). After 24 and 48 h of culture, MTS was added to a 96-well plate, and the cells were cultured for 1 h at 37 °C. The absorbance was measured in a microplate reader (BioTek EPOCH).

2.7.2. The apoptosis experiment of A549, Beas-2B and MRC-5

The effects of CS ionic solution in different dilutions (1/2, 1/8, 1/32, 1/128 dilution) on apoptosis of A549, Beas-2B and MRC-5 was investigated using Annexin V-FITC/PI kit (4A Biotech) and flow cytometry (Beckman Coulter) analysis. A549 ($1*10^6$/well), Beas-2B ($1*10^6$/well), and MRC-5 ($1*10^6$/well) were seeded in 6-well plates, where A549 and MRC-5 were cultured in DMEM+10%FBS+1%P/S while Beas-2B was cultured in DMEM+5%FBS+1%P/S. Cells were cultured for 24 h, and then the medium was removed and replaced with CS ionic solution (The control group is complete medium.). After 48 h of incubation, the cells were trypsinized (HyClone without EDTA), Annexin-FITC was added, incubated for 5 min in the dark, and then 10 μL PI was added according to the instruction of the Annexin V-FITC/PI kit manufacture. The apoptotic ratio of the three kinds of cells was then analyzed by flow cytometry.

2.7.3. The scratch test of A549, Beas-2B and MRC-5

A549, Beas-2B, and MRC-5 were cultured in 6-well plates ($2*10^6$/well), and a 10 μl pipette tip was used to scratch through the culture well surface after the cells adhered. After that, the culture medium was changed to CS ionic solution with different dilution (1/8, 1/16, 1/32, 1/64, and 1/128 dilution in serum-free medium). The control group was serum-free medium. A549 and Beas-2B were observed at 0 h, 24 h and 48 h. MRC-5 was observed at 0 h, 6 h, 12 h, 24 h and 48 h. The percentage of wound healing (Wound healing percentage = (initial wound area-wound area at a certain point in time)/initial wound area) was calculated.

2.7.4. Evaluation of the effect of CS ionic solutions on the secretion of cytokines by macrophages by ELISA

The RAW 264.7 cells with a density of $2*10^5$/well were cultured in 6-well plates, and after cell adhesion the medium was replaced with CS ionic solution in different dilutions (1/8, 1/16, 1/32, 1/64, and 1/128). The cell culture supernatant was collected after 72 h. Then, ELISA was used to detect the anti-inflammatory factors (TGF-β and IL-10) and pro-inflammatory factors (TNF-α, IL-6 and IL-1β). (NeoBioscience Technology, China) The complete medium was used as a control.

2.7.5. The analysis of $CD4^+$ T cell differentiation by flow cytometry

The RAW 264.7 cells with a density of $2*10^5$/well were cultured in 6-well plates, and after cell adhesion the medium was replaced with CS ionic solution in different dilutions (1/8, 1/16, 1/32, 1/64, and 1/128). The cell culture supernatant was collected after 72 h, and labeled as CM-control, CM-1/8CS, CM-1/6CS, CM-1/32CS, CM-1/64CS and CM-1/128CS. The complete medium was used as a control.

The naïve T cells were sorted from mouse monocytes by using mouse CD4 (L3T4) magnetic bead antibody, which was close to 100% purity (Fig. S2). CD28 mouse antibody (BioCell) was added into 6-well plates and incubated for 2 h. Then, the solution was removed and naïve T cells were added into the well, followed by the addition of CS ionic solution with different dilutions (1/8, 1/16, 1/32, 1/64, and 1/128), or supernatant of macrophage cultured with CS ionic solutions (CM-control, CM-1/8CS, CM-1/16CS, CM1/32CS, CM-1/64CS, CM-1/128CS).

Meanwhile, naïve T cells were also activated by adding CD3 mouse antibody (BioCell), and collected after 48 h stimulation. Then, surface staining with anti-mouse CD4-FITC was performed. After fixation and membrane rupture, cells were intracellularly stained with anti-mouse IFNγ-APC, IL17-PE, or mouse FOX-P3-APC (eBioscience, USA), and the stained cells were analyzed by flow cytometry.

2.8. Detection of cytokines and chemical factors in mouse BALF

On day 7 and day 21 after BLM modeling, mouse BALF supernatants were collected (5 mice per group). The cytokines in mouse BALF was analyzed using liquid suspension chip technology, including IL-1α, IL-1β, IL-2, IL-3, IL-4, IL-5, IL-6, IL-9, IL-10, IL-12 (p40), IL-12 (p70), IL-13, IL-17A, Eotaxix (CC chemokine subfamily of eosinophil chemotactic proteins), G-CSF, GM-CSF, INF-γ, KC (CXCL1), MCP-1 (monocyte chemoattractant protein 1 CCL2), MIP-1β (Macrophage inflammatory protein-1β CCL4), RANTES (regulated on activation, normal T cell expressed and secreted CCL5), TNF-α (Bio-Plex Mouse Cytokine 23-Plex).

2.9. Data analysis and processing

Graphpad prism 6 was used to process the data, which were expressed as mean ± standard deviation. The two groups were compared by independent sample T-test, and the comparison between multiple groups was by one-way analysis of variance, Fisher's LSD multiple tests, and post-test. The survival curve was drawn by Kaplan-Merier method, and the survival time was compared by log-rank test. When $P < 0.05$, it is statistically significant.

3. Results

3.1. The effect of CS ionic solution on the mortality of pulmonary fibrosis mice

Mortality of mice is a key indicator to measure the success of the pulmonary fibrosis model establishment and the effectiveness of the

therapy. Therefore, we first explored the effect of the CS ionic solution on the mortality of BLM-induced lung fibrosis mouse. The results showed that the mortality of mice in BLM + PBS was 80%, which is in accordance with that reported in the literature [35,36] and indicates a success establishment of the BLM model. Interestingly, we found that with the CS ionic solution treatment the mortality of the mice was significantly decreased as compare to the control (BLM + PBS), while no significant difference between the BLM + CS and BLM+1/8CS groups was observed (Fig. 1B). The CS ionic solution treatment reduced the mortality of fibrotic mice from 76.92% to 47.83% as compared to the control group. In addition, we also found that the original CS ionic solution and its 1/8 dilution had no negative effect on the healthy mice, and the mortality was 0% (Table S3).

3.2. The effect of CS and 1/8CS ionic solutions on BLM-induced acute inflammation and fibrosis of lung tissue in mice

The pathophysiological process of BLM-induced mouse lung fibrosis is mainly divided into two stages: early inflammation and late lung fibrosis. We used H&E and Masson staining of lung tissue to evaluate the degree of lung inflammation and fibrosis. The H&E staining revealed that on D7 and D21 after BLM modeling, the alveolar structure in the pathological section of the mouse lung tissue was significantly destroyed, and the lung interstitial inflammatory cells were infiltrated (Fig. 1C). However, as compared with that in the BLM + PBS group, the lung tissue inflammation in the BLM+1/8CS and BLM + CS groups was significantly reduced, and the results of the ALI score were also lower (Fig. 1C and D). On D7, it is clear to see that the inflammation in the BLM+1/8CS and BLM + CS groups was significantly lower than that in BLM + PBS group. On D21 after BLM modeling, the repair of lung injury seems started. The histological images showed that, as compared with the mice in the BLM + PBS group, the inflammation in the lung tissues of the mice in the BLM+1/8CS group and the BLM + CS group revealed a clear tendency of alleviated inflammation. The ALI score of the BLM + CS group was significantly lower than that of the BLM + PBS group ($P = 0.03$). Although the ALI score of the BLM+1/8CS group was not significantly different from that of the BLM + PBS group, a downward trend is visible. On D7 and D21 after modeling, the histological observation showed that the lung tissues of the mice in the PBS+1/8CS group and PBS + CS group also had a certain degree of inflammation. A small amount of inflammatory cell infiltration in the lung tissue was observed, but the corresponding ALI score was not significantly different from that of the PBS + PBS group. At the same time, the mice in the PBS + CS and PBS+1/8CS groups did not die during the observation period of the mortality experiment, which proved that the administration of CS ionic solution through the trachea is safe and feasible.

In order to further evaluate the degree of lung fibrosis, Masson staining was performed on lung tissue sections (Fig. 2A). The results showed obvious collagen deposition in lung tissues of mice after BLM modeling, which was more obvious on day 21 than on day 7. The results of the fibrosis score (Fig. 2B) also confirmed that the fibrosis on D21 was higher than that on day 7 after BLM modeling. On day 21, the degree of lung fibrosis in both BLM+1/8CS group ($P = 0.003$) and the BLM + CS group ($P = 0.006$) was clearly lower than that in the BLM + PBS group, and the fibrosis score was also significantly lower than that of BLM + PBS (Fig. 2A and B). In contrast, on day 7 after BLM modeling, a small amount of collagen deposition in the lung tissue was observed in the BLM + PBS group, and no significant difference in the degree of lung fibrosis between the CS intervention groups (BLM+1/8CS, BLM + CS) and the control group (BLM + PBS), and there was also no significant difference in fibrosis score among all groups (Fig. 2A and B), suggesting a time dependent effect of CS ionic solutions. Moreover, the quantitative results of hydroxyproline measurement are consistent with the trend of the fibrosis scores (Fig. 2C). On day 7 after BLM modeling, no difference in hydroxyproline content in the lung tissue of mice in the BLM+1/8CS and BLM + CS groups was observed as compared with that in the BLM + PBS group. But on day 21, the content of hydroxyproline in the lung tissue of mice in the BLM+1/8CS and BLM + CS groups was significantly reduced as compared with the BLM + PBS group.

The above results indicate that both the original CS ionic solution and the 1/8 dilution can significantly reduce the inflammation and fibrosis, and reduce the mortality of mice.

3.3. The effect of CS ionic solution on inflammatory cell count in BALF of mice

The inflammatory cell count in BALF is an important indicator to measure lung inflammation. To further verify the effect of CS ionic solution on lung inflammation, we collected mouse alveolar lavage fluid and performed inflammatory cell sorting and counting by flow cytometry. The cell sorting details are shown in Fig. S3.

The results showed that, in the two treatment groups (BLM + CS and BLM+1/8CS), the total number of inflammatory cells was significantly reduced on day 7 and day 21 as compared to the control group (BLM + PBS) (Fig. 3A). When we look at different inflammation cell types, it is clear to see that, as compared with the BLM + PBS group, the number of macrophages in the BLM+1/8CS group on both day 7 and 21 was significantly reduced (Fig. 3B). But there was no significant difference in the number of other types of inflammatory cells such as lymphocytes and neutrophils (Fig. 3C–E). However, in the BLM + CS group, the number of all types of inflammatory cells was significantly decreased (Fig. 3B–E). Both the number of macrophages (Fig. 3B) and $CD3^+CD8^+$ T cells (Fig. 3C) in the BLM + CS group on both day 7 and 21 was significantly less than that in the BLM + PBS group. For the $CD3^+CD4^+$ T cells on day 7, there was no significant difference between the BLM + CS group and the BLM + PBS group. However, on day 21 the number of cells in the BLM + CS group was significantly reduced as compared to the BLM + PBS group (Fig. 3D). For the neutrophils, it can be found that on day 7, the number of cells in the BLM + CS group was significantly reduced as compared to the BLM + PBS group, but there was no significant difference on day 21 (Fig. 3E). The above results prove, from the perspective of inflammatory cells, that CS ionic solution can alleviate the acute inflammation caused by BLM.

When we compare the effect CS ionic solution in different dilution, further analysis revealed that the total number of inflammatory cells in the BLM + CS group was clearly less than that in the BLM+1/8CS group on day 21 after the BLM modeling. Cell sorting results showed that the number of neutrophils in the BLM + CS group on day 7 was less than that in the BLM+1/8CS group. On day 21, the number of $CD3^+CD8^+$ T cells and $CD3^+CD4^+$ T cells were less than that in the BLM+1/8CS group (Fig. 3B–E). The above results suggest that the effect of CS ionic solution is concentration dependent, and CS solution has a more obvious inhibitory effect on inflammation than 1/8 CS dilution.

3.4. The effect of CS ionic solution on the cell viability, migration, and apoptosis of A549, Beas-2B and MRC-5 cells

It is well known that the cell viability and migration of alveolar (A549) and bronchial epithelial (Beas-2B) cells are important steps for the repair of lung tissue after injury, thereby reducing lung fibrosis, while the cell viability and migration of fibroblasts (MRC-5) may aggravate lung fibrosis. In order to further explore the mechanism of CS ionic solution on pulmonary fibrosis, we investigated the cell viability, migration, and apoptosis of three types of lung tissue cells (A549, Beas-2B and MRC-5) in the presence of CS ionic solution.

In order to determine whether CS ionic solution affects the cell viability of A549, Beas-2B and MRC-5, three groups of cells were cultured for 24 and 48 h with different dilution ratios of CS ionic solution (1/2, 1/4, 1/8, 1/16, 1/32, 1/64, 1/128).

The results showed that the CS ionic solution in certain dilution range has activity to stimulate A549 cell viability (Fig. 4A). After 48 h incubation, the cell viability rate in 1/8, 1/16, 1/32 and 1/64 dilutions

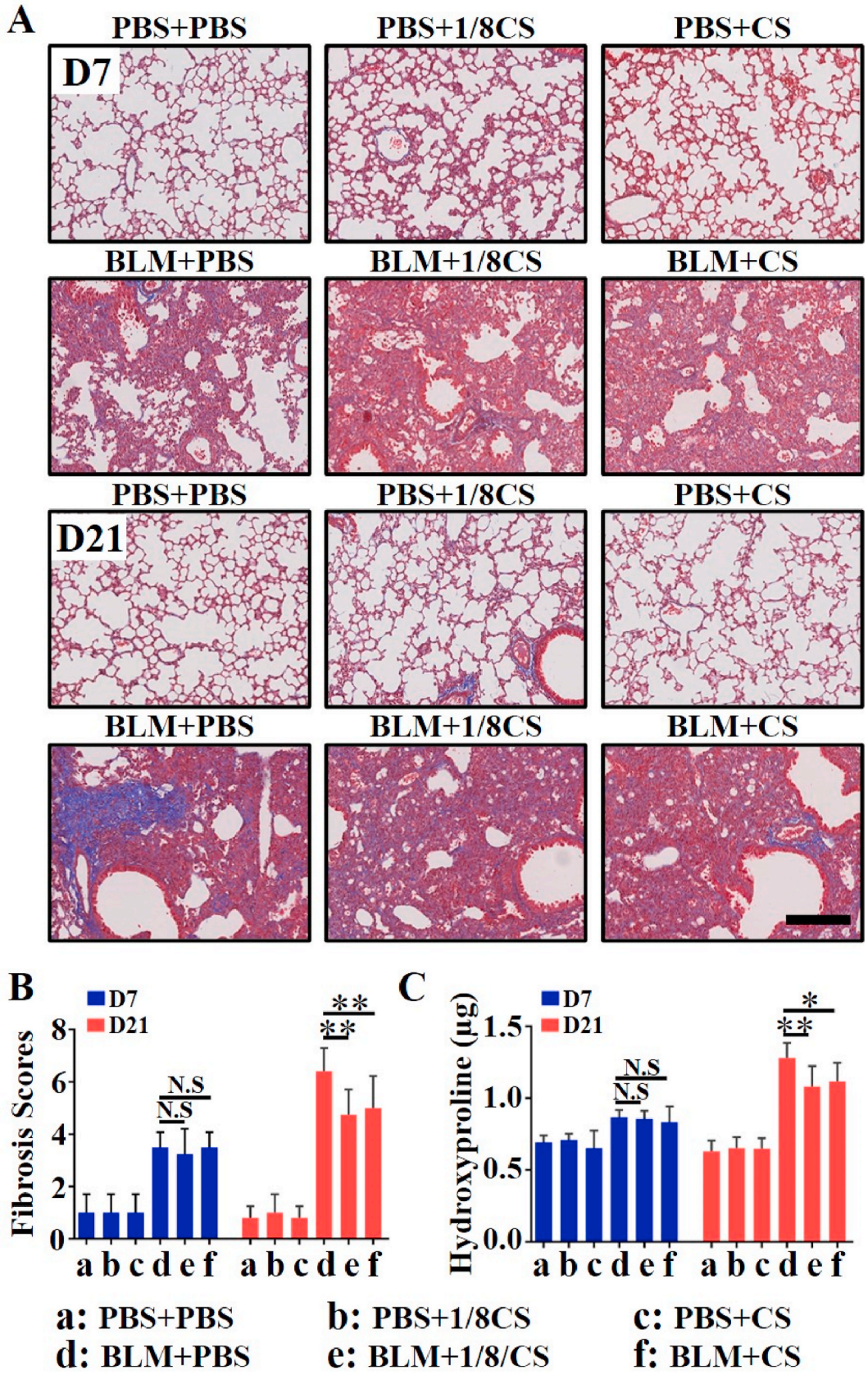

Fig. 2. The effect of CS or 1/8CS ionic solution on BLM-induced lung fibrosis in mice. (A) Masson stained images of mouse lung tissue sections on D7 and D21. (Scale = 200 μm). (B) Results of lung fibrosis score. (C) Quantitative results of hydroxyproline. (n = 5, *P < 0.05, **P < 0.01).

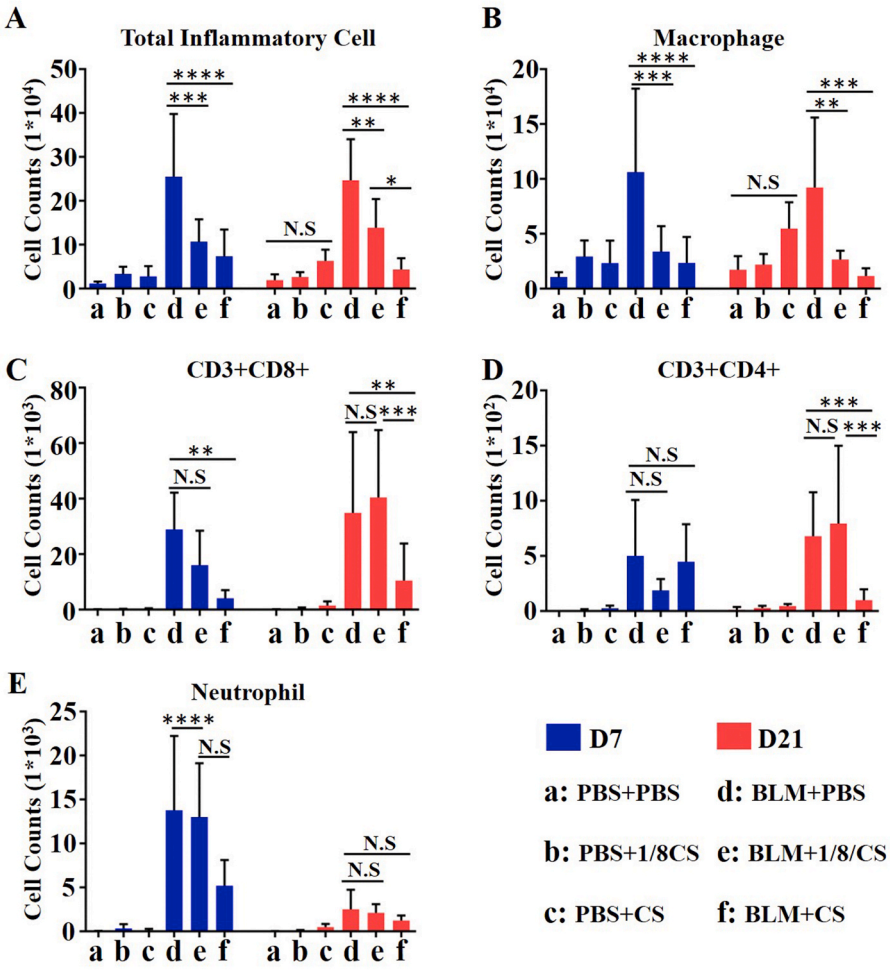

Fig. 3. The number of various types of inflammatory cells in BALF after the treatment of lung fibrosis mice with CS or 1/8CS ionic solution. (A) Total inflammatory cell count in BALF of mice on D7 and D21. (B) Count of macrophages, (C) $CD3^{+}CD8+$T lymphocytes, (D) $CD3^{+}CD4+$T lymphocytes, and (E) neutrophils in BALF of mice on D7 and D21. (n = 5, *P < 0.05, **P < 0.01, ***P < 0.001, ****P < 0.0001).

of the CS ionic solution were significantly higher than that of the control group, while in lower concentration range (1/128 dilution) no stimulation was observed. Similarly, it is observed that 1/8, 1/16 and 1/32 dilutions of the CS ionic solution also stimulated the cell viability of Beas-2B cells as compared to the control group. However, CS ionic solution did not show any stimulation on the cell viability of MRC-5 cells and at higher concentration (1/2 dilution) a minor inhibition of cell growth was evident (Fig. 4A). Above results demonstrated that the concentration (dilution) of the ionic solution is critical for the positive and negative effects. Therefore, in order to further clarify the safety of CS ionic solutions on lung tissue cells, we further investigated the cell apoptosis of these three types of cells in same dilution range of the CS ionic solution. The results showed that the apoptosis ratio of A549, Beas-2B and MRC-5 cells in 1/8, 1/32 and 1/128 dilutions of CS ionic solution was not significantly different from that of the control group, but high concentrations of CS ionic solution (1/2 dilution) caused apoptosis of the three cells (Fig. S4), which possibly due to its high pH value [37,38].

Considering the cell viability activity of CS ionic solutions in the 1/8-1/32 dilution range for A549 and Beas-2B, we selected this dilution range of the CS ionic solution for evaluation of cell migration. The results showed that the treatment with 1/8 dilution of the CS ionic solution for 24 h and the 1/8 and 1/16 dilution for 48 h promoted the migration of A549 cells. Furthermore, the treatment with CS ionic solution in 1/8-1/32 dilution range for 48 h significantly promoted the migration of Beas-2B. However, for MRC-5 cells, similar as cell viability, the treatment of CS ionic solution for 24 h and 48 h did not affect cell migration (Fig.4B and Figs. S5–S7).

The above results indicate that 1/8CS-1/32CS ionic solution can promote the cell viability and migration of alveolar (A549) and bronchial epithelial (Beas-2B) cells, but does not cause apoptosis, while the corresponding concentration does not promote the cell viability and migration of fibroblasts (MRC-5).

3.5. *CS ionic solution regulates the secretion of cytokines by macrophages*

Macrophages are the key immune cells in the process of pulmonary fibrosis, which can regulate inflammation and pulmonary fibrosis processes by secreting anti-inflammatory factors (TGF-β and IL-10) and pro-inflammatory factors (TNF-α, IL-6 and IL-1β) [1]. In order to explore the effect of CS ionic solution on the secretion of inflammatory factors by macrophages, we used CS ionic solution in different dilutions to stimulate macrophages and analyzed secretion of inflammatory factors in the culture medium. The results showed that the CS ionic solution in all three different dilutions (1/8, 1/16, 1/32) inhibited the TNF-α secretion in macrophages (Fig. 5A). However, no significant difference of TGF-β and IL-10 secretion was observed as compared with the control group after stimulation with CS ionic solution (Fig. 5B and C), while IL-6 and IL-1β could not be detected (data not shown). The above results indicate that CS ionic solution did not activate expression of cytokines such as IL-10, TGF-β, IL-6, IL-1β, but inhibit the secretion of TNFα.

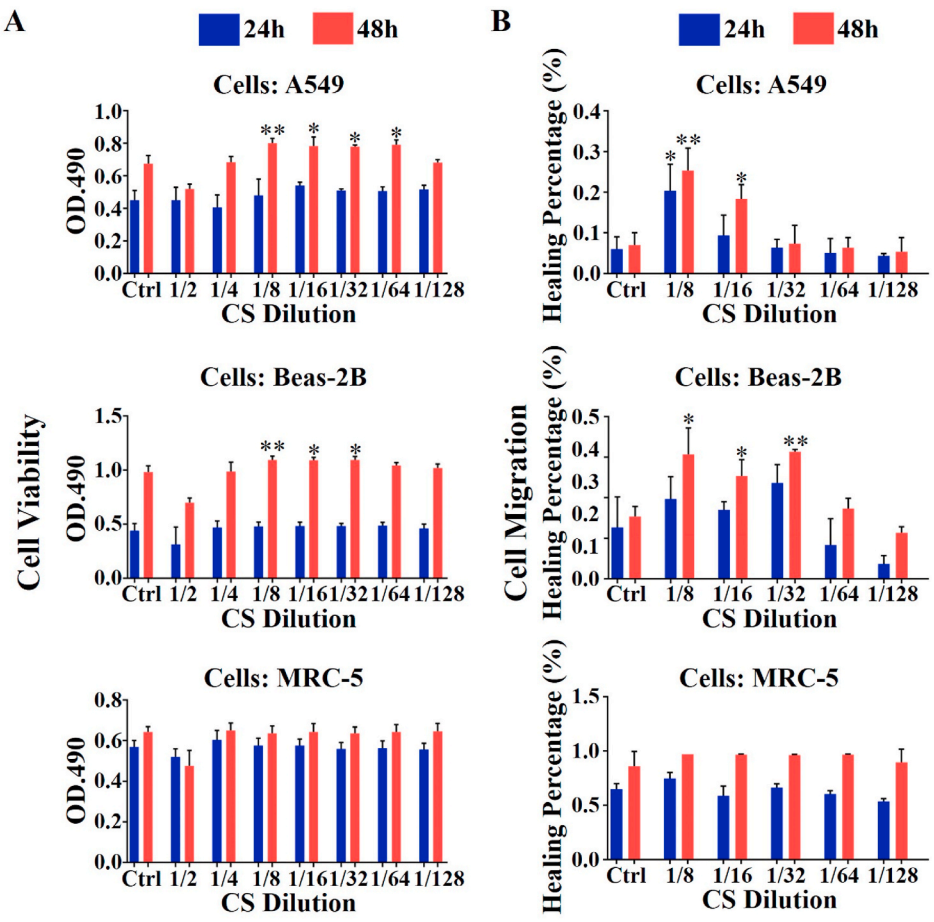

Fig. 4. The effect of different concentrations of CS ionic solution on the cell viability (A) and migration (B) of A549, Beas-2B and MRC-5. (n = 4, *P < 0.05, **P < 0.01, ****P < 0.0001).

3.6. The effect of the CS ionic solution on the concentration of inflammatory factors in mouse BALF

It is known that large amounts of macrophages exist in the alveoli, which can affect pulmonary fibrosis by secretion of inflammatory factors through paracrine mechanisms. To verify the effect of the CS ionic solution on inflammatory factors secretion in the mouse model, we collected the supernatant of mouse alveolar lavage fluid on day 7 and day 21 after BLM modeling. Liquid-phase suspension chip technology was used to screen the concentration of various inflammatory factors in mouse BALF. Inflammatory factors in BALF can be divided into two categories. One type is pro-inflammatory factors that promote inflammation including TNFα, IL-6, G-CSF, MIP-1α and KC. The other type is represented by IL-1α, which promotes the cell viability of fibroblasts and the synthesis of collagen. The results showed that among the pro-inflammatory factors, the concentration of TNF-α showed significant difference between control and experimental groups. On day 7 and 21, in the BLM + CS group and BLM+1/8CS group, the concentration of inflammatory factor TNF-α was significantly lower than that in the BLM + PBS group (Fig. 5D). The concentration of other pro-inflammatory factors also decreased significantly on day 7, but no significant difference on day 21 (Fig. 5E–H). In addition, on day 7, the concentration of the pro-fibrotic inflammatory factor IL-1α in the BLM + CS group (Fig. 5I) and the BLM+1/8CS group (Fig. 5I) was significantly lower than that in the BLM + PBS group. The above results indicate that CS ionic solution can inhibit the secretion of pro-inflammatory factors in the early inflammation stage of the fibrosis process, reduce the inflammatory response, and thereby reduce fibrosis. At the same time, it may inhibit the activity of fibroblasts by reducing the concentration of IL-1α.

3.7. Regulation of naïve T cells by the CS ionic solution

The differentiation of $CD4^+$ T cells is an important process of adaptive immunity involved in pulmonary fibrosis. $CD4^+$ T cells can differentiate into different types of cells under different stimuli, including TH1, TH2, TH17 and Treg. Among them, TH2 and TH17 can promote pulmonary fibrosis, TH1 can counter the TH2 response to reduce pulmonary fibrosis, and Treg can promote fibrosis in the early stage of pulmonary fibrosis [2]. In order to further explore how CS ionic solution is involved in immune regulation in pulmonary fibrosis, we compared the direct stimulation of CS ionic solution and indirect stimulation by CS stimulated macrophages to explore its regulatory effect on Naïve T cell differentiation.

The results showed that the CS ionic solution can indirectly inhibit the differentiation of Naïve T cells into Treg through macrophages, while no direct stimulation on Naïve T cell differentiation was observed (Fig. 6A). It is clear to see that the proportion of Treg cells in the indirect stimulation group (CM-1/32 and CM-1/128CS) was significantly lower than that in the CM group. However, in direct culture group with CS ionic solution no significant difference in Treg numbers was observed (Fig. 6B and C). In addition, we found that the direct and indirect stimulation of CS ionic solution had no effect on the differentiation of Th1 and Th17 cells (Fig. S8). Further animal experiments also confirmed above observation. In the animal model of pulmonary fibrosis, the Treg cells in BALF were sorted by flow cytometry on day 7 after BLM modeling. It is found that the proportion of mouse Treg in the BLM+1/8CS group to $CD4^+$ T cells was significantly reduced as compared to the BLM + PBS group (Fig. 6D). However, on day 21, the proportion of Treg cells in the BLM+1/8CS and BLM + CS groups was not significantly

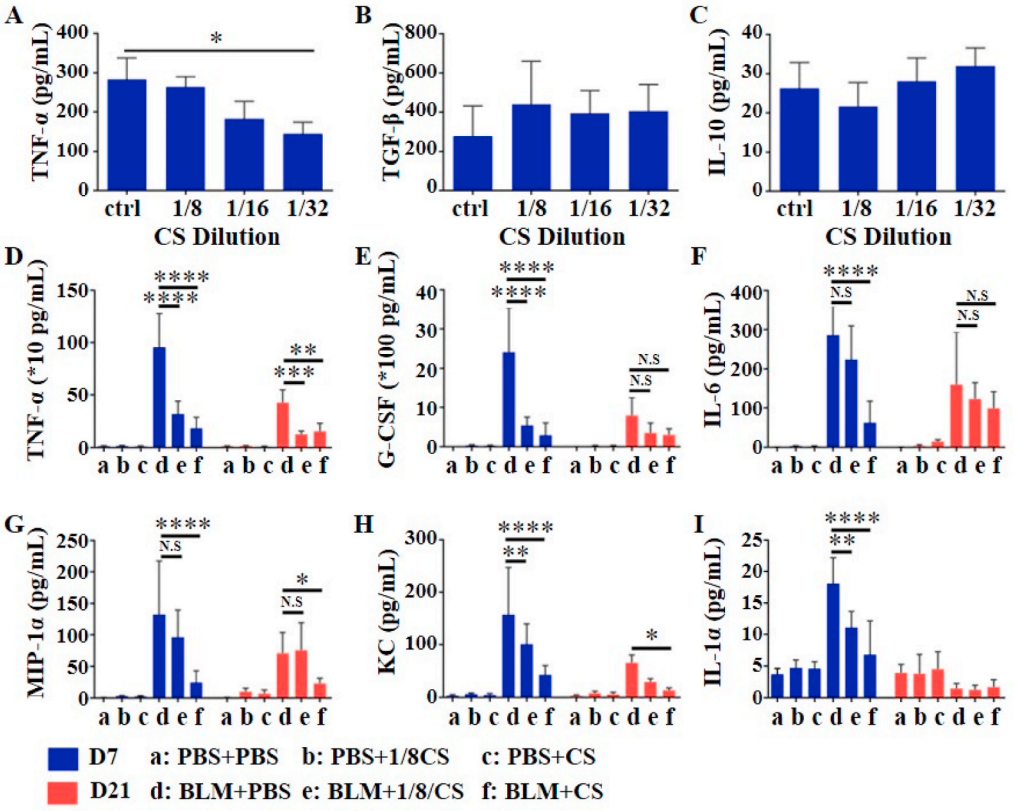

Figure 5. (A–C) ELISA detects the concentration of TNF-α (A), TGF-β (B) and IL-10 (C) after stimulating Raw 264.7 with different concentrations of CS ionic solution. (D–I) Analysis of inflammatory factors (TNFα(D), G-CSF(E), IL-6(F), MIP-1α(G), KC(H) and IL-1α (I)) in BALF of BLM-induced lung fibrosis mice after the treatment with 1/8 CS or CS ionic solutions on D7 and D21. (n = 5, *P < 0.05, **P < 0.01, ***P < 0.001, ****P < 0.0001).

different from the BLM + PBS group. This indicates that CS ionic solution may directly act on macrophages in the early stage of pulmonary fibrosis, which indirectly inhibit Treg differentiation to achieve immune regulation and reduce pulmonary fibrosis.

3.8. The ion concentration of the CS ionic solution

In order to determine the effective concentration of SiO_3^{2-} ions in the CS ionic solution, we further measured the ion concentration of the solution by ICP-AES. It can be found that the concentration of SiO_3^{2-} ions extracted by DMEM culture medium is 114.6 μg/mL, and that extracted by PBS buffer saline is 157.6 μg/mL (Table S1). Based on this result, the bioactive concentration of SiO_3^{2-} ions in the CS ionic solutions for in vivo experiments is 19.7–157.6 μg/mL, and for in vitro experiments is 3.58–14.3 μg/mL. The highest bioactive ion concentrations in vivo were about between 10 times higher than that in vitro.

4. Discussion

Pulmonary fibrosis is a progressive fatal lung disease without effective therapeutic drugs, and it is urgent to develop new therapies [10]. Inspired by the bioactivity of SiO_3^{2-} ions derived from silicate bioceramics in regulating activities of different type of cells such as tissue-specific endothelial and epithelial cells, stem cells and immune cells [19,39,40] and enhancing soft tissue regeneration [20,41], we speculate that the CS ionic solution containing silicate ions may have a regulatory effect on the alveolar epithelium and its local immune microenvironment, which might be beneficial to repair the lung injury and inhibit pulmonary fibrosis. Our experimental results confirmed this hypothesis that the CS ionic solution in certain concentration range indeed significantly inhibited the progress of acute inflammation and pulmonary fibrosis of lung tissue induced by BLM. More interestingly, we found that the treatment of CS ionic solutions significantly reduced BLM animal mortality. In our previous work, it was found that the CS ionic solution did not have any acute toxicity to healthy mice within 28 days (intravenous administration). Since we applied CS ionic solution by inhalation, when the ionic solution enters the lung, it may further enter the blood circulation through the capillaries [42]. According to our previous research, after entering the blood circulation, the silicate ions will be excreted in the form of urine and will not accumulate in heart, lungs, liver, and kidneys [19]. In this study, compared with the control group, the mortality of pulmonary fibrosis mice decreased from 76.92% to 47.83%, while the mortality of healthy mice was 0% (tracheal inhalation administration). Although the method of CS solution administration in this study is different as that in our previous study for cardiac tissue repair, our results confirmed the safety of the CS ion solution in the concentration range from original extracts to 1/8 dilution. Furthermore, in our previous studies we have found that the bioactivity of silicate ions is often in a broad concentration range [19,32]. In the present study, we have indeed found that cell responses are concentration dependent and for different cell types the bioactive concentration ranges are different, such as for A549 cells the bioactive range is 1/8 to 1/64 dilutions, and for Beas-2B cells are 1/8 to 1/32 dilutions. Considering the different environments, the in vivo bioactive concentration range could be significantly different as compared to the in vitro situation. In our in vivo experiments, we first selected two concentrations and found that no significant difference in the therapeutic effects of the two solution concentrations. This result suggests that 1/8 dilution already reaches the maximal bioactive concentration for in vivo situation, but the minimal bioactive concentration is still unknown, and needs to be evaluated in future.

Alveolar epithelial cell injury, abnormal activation of macrophages

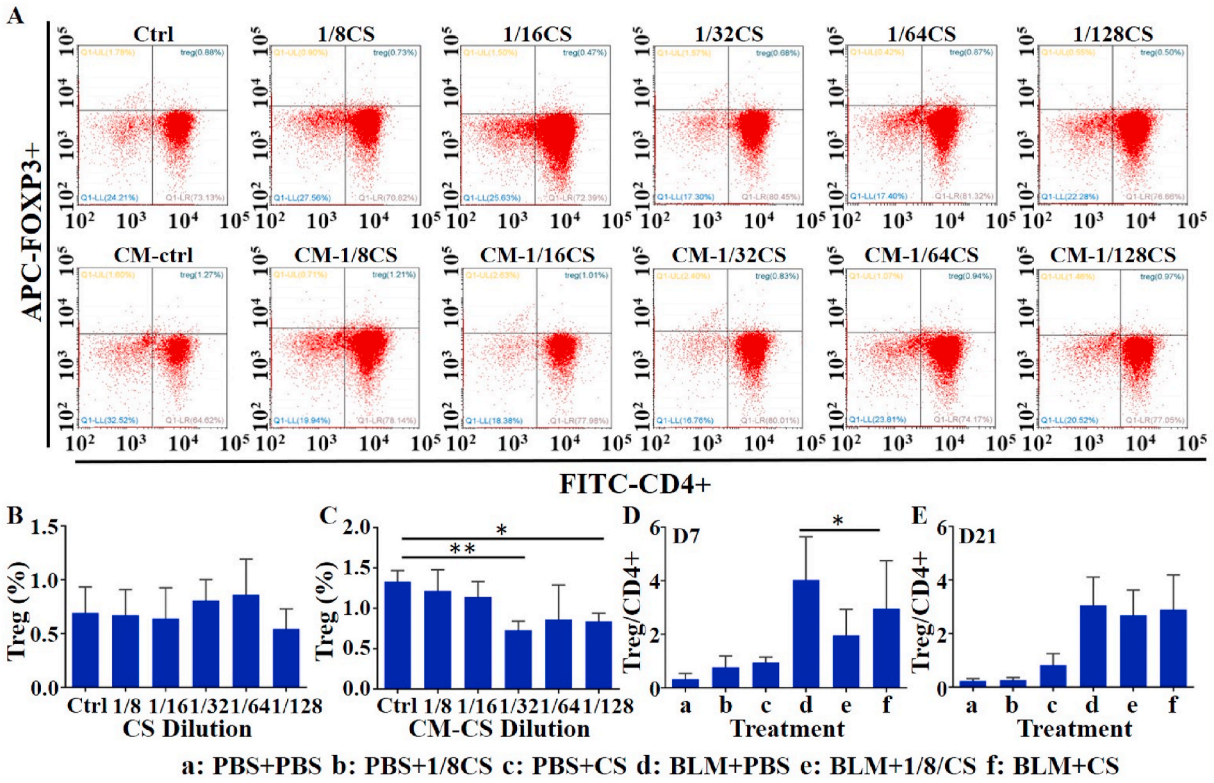

Fig. 6. Flow cytometry analysis of cells after treatment with different concentrations of CS ionic solution directly or indirectly affect the differentiation of naïve T cells into Treg (Directly affect the differentiation (CS): Lymphocytes were cultured by using CS solution.; Indirectly affect the differentiation (CM-CS): Lymphocytes were cultured through the supernatant (CS solution) produced by culturing macrophages for 72 h). (A) The proportion of Treg cells. (B) The proportion of Treg cells in the direct stimulation group. (C) The proportion of Treg cells in the indirect stimulation group. (n = 4) (D, E) On D7 (D) and D21 (E) days after BLM modeling, cells in mouse BALF were collected and the proportion of Treg was detected by flow cytometry.

and cell viability of fibroblasts are important pathological mechanisms of pulmonary fibrosis [43]. In recent years, basic research on the treatment of pulmonary fibrosis is mainly focusing on the regulation of fibroblast cell viability and extracellular matrix secretion [44,45], while less attention is paid on alveolar epithelial cell injury, which is however an important step in the initiation of pulmonary fibrosis. Our previous studies have shown that the ionic solutions of silicate bioceramics can significantly stimulate the cell viability and migration of human umbilical vein endothelial cells and skin epidermal cells, enhance the activity of epidermal cells and promote the repair of skin damage [21]. Therefore, we think that the alveolar epithelial cell injury may be considered as a target for preventing lung fibrosis, and our hypothesis is that the SiO_3^{2-} released from bioactive silicate bioceramics may activate alveolar epithelial cells (A549) and bronchial epithelial cells (Beas-2B) to repair lung injury. To verify our hypothesis, we explored the effects of CS ionic solution on A549 and Beas-2B cells, and confirmed that 1/8-1/32 dilutions of CS ionic solution indeed effectively promoted the cell viability and migration of A549 and Beas-2B, while fibroblasts (MRC-5) cell viability was not affected by CS ionic solutions within this concentration range. In our previous work, we have noticed the selective effects of CS ionic solutions on different cells and cellular functions, and the effects are time dependent [32,38]. We found that the viability of human dermal fibroblasts was greatly improved after 7 days of treatment with CS ionic solution [46]. In this study, we did not observe stimulatory effect on MRC-5 cell viability probably due to insufficient treatment time, because primarily we considered to evaluate the early-stage effect and treated cells with CS solutions only for 48 h, but the observed result for 48 h is in consistence with a study of the CS solutions on the viability of human periodontal ligament fibroblasts for same culturing time [47].

Indeed, we found in this study that the CS ionic solution inhibited the overexpression of collagen in vivo, but it is not clear whether MRC-5 expressed low level collagen, or the expression of enzymes such as MMPs for collagen degradation was up-regulated. A previous study has shown that silica nanoparticles can up-regulate matrix metalloproteinases (MMPs) and down-regulate tissue inhibitors of MMPs (TIMPs) to promote collagen degradation and inhibit liver fibrosis [48]. Therefore, one possible effect of the CS ion solution might also be the regulation of MMPs and TIMPs expression. Furthermore, previous studies revealed that silica nanoparticles can activate some signaling pathways on epithelia cells, but not fibroblasts. It is found that the pulmonary epithelial cells are activated by silica nanoparticles through regulating the ERK pathway [49], but not MRC-5 [50]. Some studies also revealed that silica nanoparticles may be degraded by release Si ions [51]. Therefore, it is possible that the CS ionic solutions may also activate epithelia cells such as A549 and Beas-2B through the ERK pathway.

In addition to the alveolar epithelial cell injury, it is known that changes in the local immune microenvironment of lung tissue can affect the process of pulmonary fibrosis [52]. In the early stage of BLM-induced pulmonary fibrosis, BLM caused AEC2 damage and inflammation, which activated an immune response dominated by macrophages. This leads to the accumulation of large number of immune cells such as neutrophils, macrophages and T lymphocytes in the lung interstitium and alveolar cavity, which participate in the process of alveolar epithelial injury and lung fibrosis [53]. In the present study, we found that the CS ionic solution significantly reduced the number of macrophages as well as other types of inflammatory cells, including T cells ($CD8^+$ and $CD4^+$) and neutrophils in bronchoalveolar lavage fluid (BALF). In order to further explore the immunomodulatory effect of CS ionic solution, we investigated the secretion of the inflammatory factors in BALF, and found that CS and 1/8CS ionic solution treatment indeed reduced the concentration of TNF-α, MIP-1α, IL-6, KC, G-CSF and IL-1α.

Among these inflammatory factors, TNF-α, MIP-1α, IL-6, KC and G-CSF can promote the differentiation and maturation of monocytes and neutrophils, be accumulated in lung tissue by chemotaxis and aggravate lung injury and fibrosis in the process of lung fibrosis [54], while IL-1α can directly act on fibroblasts to promote their cell viability and collagen synthesis [55]. Our previous study has shown that ionic solution of silicate bioceramics may reduce the expression of some inflammatory factors such as TNF-α、MIP-1α、IL-6 and IL-1β, and possible mechanisms might be related to the enhanced macrophage apoptosis and inhibition of macrophages to express these factors [54]. Therefore, it can be speculated that one of the main explanations for the immunoregulatory effect of the CS ionic solution might be the regulation of macrophages, stimulation of cell apoptosis and inhibition of the secretion of various inflammatory factors, which resulted in the decrease of total inflammatory cells. Interestingly, although these inflammatory indexes decreased significantly on day 21, the ALI scores representing early pathological changes did not decrease significantly. This may be due to the reason that pulmonary fibrosis process involves cellular interactions via a complex cytokine-signaling mechanism with different inflammatory and pathological changes [56]. Our previous studies have shown that the CS ionic solution may stimulate different type of cells slowly in some wound repair situation [19,27]. Therefore, we assume that CS ionic solution might act not as fast as biomolecules and need more time to affect all the fibrosis related parameters. However, further studies are required to confirm this assumption.

Another possible explanation of the immunomodulation mechanism of the CS ionic solution on pulmonary fibrosis might be the inhibitory effect of CS ionic solution on TNFα expression and the differentiation of naïve T-cell to Treg cells. Studies have shown that TNFα can significantly promote the differentiation and cell viability of Treg cells [57,58], and the increase of Treg in the early inflammatory phase will promote BLM-induced pulmonary fibrosis. In the early inflammation stage, adoptive transfer of Treg cells to fibrosis model mice also aggravates lung fibrosis [59]. In contrast, the use of monoclonal antibodies to eliminate Treg can reduce BLM-induced pulmonary fibrosis [60]. Furthermore, the reduction of Treg cells may inhibit Th2 related immune response and reduce fibrosis [59]. Our in vivo experimental results showed that, after CS ionic solution treatment, the concentration of TNFα was significantly reduced. The results of in vitro experiments also show that CS ionic solution reduced the TNF-α concentration and the number of Treg cells. Therefore, we speculate that the CS ionic solution inhibits the differentiation of T cells into Tregs by inhibiting TNF-α secretion of macrophages.

It is worth to indicate that, most clinically used drugs for lung fibrosis treatment are focusing on one target, either regulating the function of alveolar epithelial cells II (AEC2) for reducing the damage, or regulating macrophages to reduce inflammation. The ionic solution treatment strategy used in this study demonstrates that the CS ionic solution simultaneously regulates two type of key cells such as alveolar epithelial cells and immune cells such as macrophages in the development of pulmonary fibrosis. It not only promotes the cell viability and migration of AEC2 required for repair of damaged tissue, but also inhibits the profibrotic inflammatory factors secreted by macrophages. Our results indicate that this bioactive ion-based therapy might affect multiple signaling pathways and systematically regulate the fibrosis process, but more studies required to confirm this assumption.

In summary, lung injury is the initiating factor of pulmonary fibrosis. Our results suggest that the CS ionic solution inhibits pulmonary fibrosis possibly through the following ways (Fig. 7). First, bioactive ions directly act on AEC2 to promote its cell viability and migration, thereby promoting the repair of lung injury. Secondly, the bioactive ions of CS ionic solution affect macrophages and inhibit the secretion of inflammatory factors such as TNF-α, and indirectly inhibit Treg differentiation and cell viability through macrophage regulation, thereby reducing the number of inflammatory cells such as neutrophils and monocytes in lung tissue, which results in the reduced lung damage.

5. Conclusions

This study demonstrated a novel treatment of pulmonary fibrosis based on ion therapy using bioactive ionic solution derived from silicate bioceramics. The bioactive ionic solution regulated the pulmonary fibrosis process through two pathways, one is the stimulation of alveolar epithelial cells to repair damaged lung tissue, and the other is the

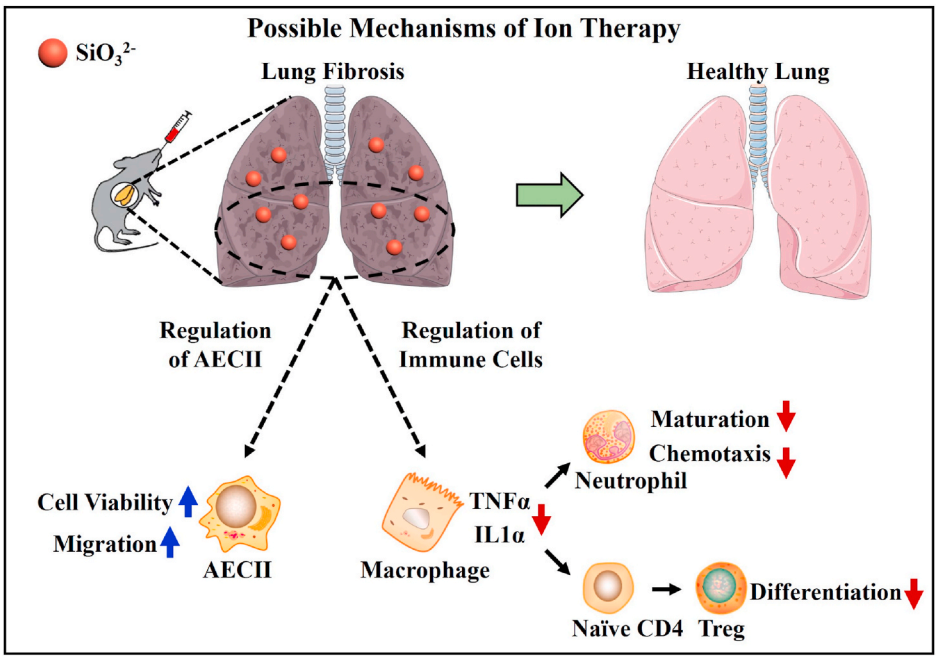

Fig. 7. The mechanism hypothesis of CS ionic solution in the treatment of lung fibrosis. SiO_3^{2-} can promote the cell viability and migration of AECII to repair lung injury and reduce lung fibrosis. SiO_3^{2-} can inhibit the secretion of inflammatory factors (IL-1α, TNF-α, etc.) of macrophages and reduce lung fibrosis. The reduction of TNFα can inhibit the maturation and chemotaxis of neutrophils, and reduce the differentiation and expansion of Treg, thereby reducing lung fibrosis.

regulation immune cells such as macrophages to inhibit inflammatory factor secretion and reduce the number of inflammatory cells such as neutrophils and monocytes in lung tissue and reduce the lung injury. This finding suggests that bioactive ions derived from silicate bioceramics might have a multi-pathway activation function and the approach of ion therapy might be an effective method for the treatment of pulmonary fibrosis.

Data availability statement

The raw/processed data forms part of an ongoing study and may be requested from the authors.

CRediT authorship contribution statement

Tao Chen: Experimental design, Formal analysis, Interpretation, Data analysis and interpretation, Manuscript writing. **Zhaowenbin Zhang:** Formal analysis, Interpretation, Data analysis and interpretation, Manuscript writing, All authors read and approved the final manuscript. **Dong Weng:** Provision of study materials, Manuscript writing. **LiQin Lu:** Experimental design, Provision of study materials, Manuscript writing. **XiaoYa Wang:** Provision of study materials, Manuscript writing. **Hui Qiu:** Formal analysis, Interpretation, Data analysis and interpretation, Manuscript writing. **MengMeng Zhao:** Formal analysis, Interpretation, Data analysis and interpretation, Manuscript writing. **Jiang Chang:** Scientific study design and manuscript revision, Manuscript writing. **Hui-Ping Li:** Experimental design, Scientific study design and manuscript revision, Manuscript writing.

Declaration of competing interest

There are no conflicts of interest in this work.

Acknowledgements

This study was financially supported by the Ministry of Science and Technology of the People's Republic of China (Grant Nos. 2016YFC1100200 and 2016YFC1100204 and 2016YFC1100201), the National Natural Science Foundation of China (Grant Nos. 81730002, 81670055, 81670056, 91442103, 81500052, 32000945 and 81570057), National Science & Technology Major Project for Key New Drug Creation and Manufacturing Program (No: 2018ZX09201002-006), National Science Foundation of Shanghai (18ZR143400) and Shanghai Family Planning Commission Health Industry Clinical Research Project (Grant No. 20184Y0084). The authors thank Professor Chen Wang for conceiving of the study and offering help for the experiment.

Appendix A. Supplementary data

Supplementary data to this article can be found online at https://doi.org/10.1016/j.bioactmat.2021.02.013.

References

[1] G. Bagnato, S. Harari, Cellular interactions in the pathogenesis of interstitial lung diseases, Eur. Respir. Rev. : an official journal of the European Respiratory Society 24 (135) (2015) 102–114.
[2] P.J. Wolters, H.R. Collard, K.D. Jones, Pathogenesis of idiopathic pulmonary fibrosis, in: A.K. Abbas, S.J. Galli, P.M. Howley (Eds.), Annual Review of Pathology: Mechanisms of Disease, Vol 92014, pp. 157-179.
[3] T. Adachi, J.-M. Chong, N. Nakajima, M. Sano, J. Yamazaki, I. Miyamoto, H. Nishioka, H. Akita, Y. Sato, M. Kataoka, H. Katano, M. Tobiume, T. Sekizuka, K. Itokawa, M. Kuroda, T. Suzuki, Clinicopathologic and immunohistochemical findings from autopsy of patient with COVID-19, Japan, Emerg. Infect. Dis. 26 (9) (2020) 2157–2161.
[4] L. Bao, W. Deng, B. Huang, H. Gao, J. Liu, L. Ren, Q. Wei, P. Yu, Y. Xu, F. Qi, Y. Qu, F. Li, Q. Lv, W. Wang, J. Xue, S. Gong, M. Liu, G. Wang, S. Wang, Z. Song, L. Zhao, P. Liu, L. Zhao, F. Ye, H. Wang, W. Zhou, N. Zhu, W. Zhen, H. Yu, X. Zhang, L. Guo, L. Chen, C. Wang, Y. Wang, X. Wang, Y. Xiao, Q. Sun, H. Liu, F. Zhu, C. Ma, L. Yan, M. Yang, J. Han, W. Xu, W. Tan, X. Peng, Q. Jin, G. Wu, C. Qin, The pathogenicity of SARS-CoV-2 in hACE2 transgenic mice, Nature 583 (7818) (2020) 830–+.
[5] M. Yu, Y. Liu, D. Xu, R. Zhang, L. Lan, H. Xu, Prediction of the development of pulmonary fibrosis using serial thin-section CT and clinical features in patients discharged after treatment for COVID-19 pneumonia, Korean J. Radiol. 21 (6) (2020) 746–755.
[6] T.E. King Jr., W.Z. Bradford, S. Castro-Bernardini, E.A. Fagan, I. Glaspole, M. K. Glassberg, E. Gorina, P.M. Hopkins, D. Kardatzke, L. Lancaster, D.J. Lederer, S. D. Nathan, C.A. Pereira, S.A. Sahn, R. Sussman, J.J. Swigris, P.W. Noble, A.S. Grp, A phase 3 trial of pirfenidone in patients with idiopathic pulmonary fibrosis, N. Engl. J. Med. 370 (22) (2014) 2083–2092.
[7] L. Richeldi, R.M. du Bois, G. Raghu, A. Azuma, K.K. Brown, U. Costabel, V. Cottin, K.R. Flaherty, D.M. Hansell, Y. Inoue, D.S. Kim, M. Kolb, A.G. Nicholson, P. W. Noble, M. Selman, H. Taniguchi, M. Brun, F. Le Maulf, M. Girard, S. Stowasser, R. Schlenker-Herceg, B. Disse, H.R. Collard, I.T. Investigators, Efficacy and safety of nintedanib in idiopathic pulmonary fibrosis, N. Engl. J. Med. 370 (22) (2014) 2071–2082.
[8] M. Ackermann, Y.O. Kim, W.L. Wagner, D. Schuppan, C.D. Valenzuela, S. J. Mentzer, S. Kreuz, D. Stiller, L. Wollin, M.A. Konerding, Effects of nintedanib on the microvascular architecture in a lung fibrosis model, Angiogenesis 20 (3) (2017) 359–372.
[9] W.C. Chen, N.J. Chen, H.P. Chen, W.K. Yu, V.Y.F. Su, H. Chen, H.H. Wu, K.Y. Yang, Nintedanib reduces neutrophil chemotaxis via activating GRK2 in bleomycin-induced pulmonary fibrosis, Int. J. Mol. Sci. 21 (13) (2020) 4735.
[10] G. Raghu, B. Rochwerg, Y. Zhang, C.A.C. Garcia, A. Azuma, J. Behr, J.L. Brozek, H. R. Collard, W. Cunningham, S. Homma, T. Johkoh, F.J. Martinez, J. Myers, S. L. Protzko, L. Richeldi, D. Rind, M. Selman, A. Theodore, A.U. Wells, H. Hoogsteden, H.J. Schuenemann, Ats, ers, jrs, alat, an official ATS/ERS/JRS/ALAT clinical practice guideline: treatment of idiopathic pulmonary fibrosis an update of the 2011 clinical practice guideline, Am. J. Respir. Crit. Care Med. 192 (2) (2015) E3–E19.
[11] P.M. George, C.M. Patterson, A.K. Reed, M. Thillai, Lung transplantation for idiopathic pulmonary fibrosis, Lancet Respiratory Medicine 7 (3) (2019) 271–282.
[12] J. Liang, Y. Zhang, T. Xie, N. Liu, H. Chen, Y. Geng, A. Kurkciyan, J.M. Mena, B. R. Stripp, D. Jiang, P.W. Noble, Hyaluronan and TLR4 promote surfactant-protein-C-positive alveolar progenitor cell renewal and prevent severe pulmonary fibrosis in mice, Nat. Med. 22 (11) (2016) 1285–1293.
[13] L.R. Young, P.M. Gulleman, C.W. Short, H. Tanjore, T. Sherrill, A. Qi, A.P. McBride, R. Zaynagetdinov, J.T. Benjamin, W.E. Lawson, S.V. Novitskiy, T.S. Blackwell, Epithelial-macrophage interactions determine pulmonary fibrosis susceptibility in Hermansky-Pudlak syndrome, Jci Insight 1 (17) (2016), e88947.
[14] C. Wu, J. Chang, A review of bioactive silicate ceramics, Biomed. Mater. 8 (3) (2013), 032001.
[15] A. Hoppe, N.S. Gueldal, A.R. Boccaccini, A review of the biological response to ionic dissolution products from bioactive glasses and glass-ceramics, Biomaterials 32 (11) (2011) 2757–2774.
[16] K. Lin, Y. Liu, H. Huang, L. Chen, Z. Wang, J. Chang, Degradation and silicon excretion of the calcium silicate bioactive ceramics during bone regeneration using rabbit femur defect model, J. Mater. Sci. Mater. Med. 26 (6) (2015) 197.
[17] Y.J. No, J.J. Li, H. Zreiqat, Doped calcium silicate ceramics: a new class of candidates for synthetic bone substitutes, Materials 10 (2) (2017) 153.
[18] C.M. Primus, F.R. Tay, L.-n. Niu, Bioactive tri/dicalcium silicate cements for treatment of pulpal and periapical tissues, Acta Biomater. 96 (2019) 35–54.
[19] M. Yi, H. Li, X. Wong, J. Yan, L. Gao, Y. He, X. Zhong, Y. Cai, W. Feng, Z. Wen, C. Wu, C. Ou, J. Chang, M. Chen, Ion therapy: a novel strategy for acute myocardial infarction, Adv. Sci. 6 (1) (2019) 1801260.
[20] Q. Yu, J. Chang, C. Wu, Silicate bioceramics: from soft tissue regeneration to tumor therapy, J. Mater. Chem. B 7 (36) (2019) 5449–5460.
[21] F. Wang, X. Wang, K. Ma, C. Zhang, J. Chang, X. Fu, Akermanite bioceramic enhances wound healing with accelerated reepithelialization by promoting proliferation, migration, and stemness of epidermal cells, Wound repair and regeneration, official publication of the Wound Healing Society [and] the European Tissue Repair Society 28 (1) (2020) 16–25.
[22] H.Y. Li, J. Chang, Stimulation of proangiogenesis by calcium silicate bioactive ceramic, Acta Biomater. 9 (2) (2013) 5379–5389.
[23] X.T. Wang, L.Y. Wang, Q. Wu, F. Bao, H.T. Yang, X.Z. Qiu, J. Chang, Chitosan/calcium silicate cardiac patch stimulates cardiomyocyte activity and myocardial performance after infarction by synergistic effect of bioactive ions and aligned nanostructure, ACS Appl. Mater. Interfaces 11 (1) (2019) 1449–1468.
[24] S. Verrier, J.J. Blaker, V. Maquet, L.L. Hench, A.R. Boccaccini, PDLLA/Bioglass (R) composites for soft-tissue and hard-tissue engineering: an in vitro cell biology assessment, Biomaterials 25 (15) (2004) 3013–3021.
[25] Y. Huang, C. Wu, X. Zhang, J. Chang, K. Dai, Regulation of immune response by bioactive ions released from silicate bioceramics for bone regeneration, Acta Biomater. 66 (2018) 81–92.
[26] X. Dong, J. Chang, H. Li, Bioglass promotes wound healing through modulating the paracrine effects between macrophages and repairing cells, J. Mater. Chem. B 5 (26) (2017) 5240–5250.
[27] Y. Zhou, C. Wu, J. Chang, Bioceramics to regulate stem cells and their microenvironment for tissue regeneration, Mater, Today Off. 24 (2019) 41–56.
[28] H.Y. Li, J. Chang, Fabrication and characterization of bioactive wollastonite/PHBV composite scaffolds, Biomaterials 25 (24) (2004) 5473–5480.
[29] Z.W.B. Zhang, Q.X. Dai, Y. Zhang, H. Zhuang, E.D. Wang, Q. Xu, L.L. Ma, C.T. Wu, Z.G. Huan, F. Guo, J. Chang, Design of a multifunctional biomaterial inspired by

ancient Chinese medicine for hair regeneration in burned skin, ACS Appl. Mater. Interfaces 12 (11) (2020) 12489–12499.
[30] V. Della Latta, A. Cecchettini, S. Del Ry, M.A. Morales, Bleomycin in the setting of lung fibrosis induction: from biological mechanisms to counteractions, Pharmacol. Res. 97 (2015) 122–130.
[31] J. Tashiro, G.A. Rubio, A.H. Limper, K. Williams, S.J. Elliot, I. Ninou, V. Aidinis, A. Tzouvelekis, M.K. Glassberg, Exploring animal models that resemble idiopathic pulmonary fibrosis, Front. Med. 4 (2017) 118.
[32] X.Y. Wang, L. Gao, Y. Han, M. Xing, C.C. Zhao, J.L. Peng, J. Chang, Silicon-enhanced adipogenesis and angiogenesis for vascularized adipose tissue engineering, Adv. Sci. 5 (11) (2018) 1800776.
[33] K. Mikawa, K. Nishina, Y. Takao, H. Obara, ONO-1714, a nitric oxide synthase inhibitor, attenuates endotoxin-induced acute lung injury in rabbits, Anesth. Analg. 97 (6) (2003) 1751–1755.
[34] R.-H. Huebner, W. Gitter, N.E. El Mokhtari, M. Mathiak, M. Both, H. Bolte, S. Freitag-Wolf, B. Bewig, Standardized quantification of pulmonary fibrosis in histological samples, Biotechniques 44 (4) (2008) 507–+.
[35] M.S. Kim, A.R. Baek, J.H. Lee, A.S. Jang, D. Kim, S.S. Chin, S.W. Park, IL-37 attenuates lung fibrosis by inducing autophagy and regulating TGF-beta 1 production in mice, J. Immunol. 203 (8) (2019) 2265–2275.
[36] Z.L. Huang, S.Q. Wang, Y.T. Liu, L.C. Fan, Y. Zeng, H.X. Han, H.Y. Zhang, X.T. Yu, Y.D. Zhang, D.D. Huang, Y.J. Wu, W.X. Jiang, P.P. Zhu, X.Y. Zhu, X.H. Yi, GPRC5A reduction contributes to pollutant benzo a pyrene injury via aggravating murine fibrosis, leading to poor prognosis of IIP patients, Sci. Total Environ. 739 (2020) 139923.
[37] M. Meenapriya, R. Sandhya, Assessment of pH of calcium silicate based root canal sealers at various time periods - an in vitro study, Biosci. Biotechnol. Res. Commun. 13 (7) (2020) 286–290.
[38] M. Xing, X.Y. Wang, E.D.A. Wang, L. Gao, J. Chang, Bone tissue engineering strategy based on the synergistic effects of silicon and strontium ions, Acta Biomater. 72 (2018) 381–395.
[39] X. Wang, L. Wang, Q. Wu, F. Bao, H. Yang, X. Qiu, J. Chang, Chitosan/calcium silicate cardiac patch stimulates cardiomyocyte activity and myocardial performance after infarction by synergistic effect of bioactive ions and aligned nanostructure, ACS Appl. Mater. Interfaces 11 (1) (2019) 1449–1468.
[40] Y. Zhang, M. Chang, F. Bao, M. Xing, E. Wang, Q. Xu, Z. Huan, F. Guo, J. Chang, Multifunctional Zn doped hollow mesoporous silica/polycaprolactone electrospun membranes with enhanced hair follicle regeneration and antibacterial activity for wound healing, Nanoscale 11 (13) (2019) 6315–6333.
[41] C. O'Leary, J.L. Gilbert, S. O'Dea, F.J. O'Brien, S.-A. Cryan, Respiratory tissue engineering: current status and opportunities for the future, Tissue Eng. B Rev. 21 (4) (2015) 323–344.
[42] K. Suresh, L.A. Shimoda, Lung circulation, Comp. Physiol. 6 (2) (2016) 897–943.
[43] J.A. Kropski, T.S. Blackwell, Progress in understanding and treating idiopathic pulmonary fibrosis, in: M.E. Klotman (Ed.), Annual Review of Medicine, Vol vol. 702019, pp. 211-224.
[44] B. Ng, J. Dong, G. D'Agostino, S. Viswanathan, A.A. Widjaja, W.-W. Lim, N.S.J. Ko, J. Tan, S.P. Chothani, B. Huang, C. Xie, C.J. Pua, A.-M. Chacko, N. Guimaraes-Camboa, S.M. Evans, A.J. Byrne, T.M. Maher, J. Liang, D. Jiang, P.W. Noble, S. Schafer, S.A. Cook, Interleukin-11 is a therapeutic target in idiopathic pulmonary fibrosis, Sci. Transl. Med. 11 (511) (2019), eaaw1237.
[45] A. Mor, M.S. Salto, A. Katav, N. Barashi, V. Edelshtein, M. Manetti, Y. Levi, J. George, M. Matucci-Cerinic, Blockade of CCL24 with a monoclonal antibody ameliorates experimental dermal and pulmonary fibrosis, Ann. Rheum. Dis. 78 (9) (2019) 1260–1268.
[46] Y. Han, Y.H. Li, Q.Y. Zeng, H.Y. Li, J.L. Peng, Y.H. Xu, J. Chang, Injectable bioactive akermanite/alginate composite hydrogels for in situ skin tissue engineering, J. Math. Chem. B 5 (18) (2017) 3315–3326.
[47] S. Kucukkaya, M.O. Gorduysus, N.D. Zeybek, S.F. Muftuoglu, In Vitro Cytotoxicity of Calcium Silicate-Based Endodontic Cement as Root-End Filling Materials, Sci. Tech. Rep. vol. 2016 (2016) 5.
[48] F. Peng, J.K. Tee, M.I. Setyawati, X.G. Ding, H.L.A. Yeo, Y.L. Tan, D.T. Leong, H. K. Ho, Inorganic nanomaterials as highly efficient inhibitors of cellular hepatic fibrosis, ACS Appl. Mater. Interfaces 10 (38) (2018) 31938–31946.
[49] Y.Q. Liu, H.Y. Wei, J. Tang, J.M. Yuan, M.M. Wu, C.J. Yao, K. Hosoi, S.L. Yu, X. Y. Zhao, Y. Han, G. Chen, Dysfunction of pulmonary epithelial tight junction induced by silicon dioxide nanoparticles via the ROS/ERK pathway and protein degradation, Chemosphere 255 (2020) 126954.
[50] S.M. Huang, X.B. Zuo, J.J. Li, S.F.Y. Li, B.H. Bay, C.N. Ong, Metabolomics studies show dose-dependent toxicity induced by SiO2 nanoparticles in MRC-5 human fetal lung fibroblasts, Advanced Healthcare Materials 1 (6) (2012) 779–784.
[51] B.W. Yang, Y. Chen, J.L. Shi, Mesoporous silica/organosilica nanoparticles: synthesis, biological effect and biomedical application, Mater. Sci. Eng. R Rep. 137 (2019) 66–105.
[52] S. Kolahian, I.E. Fernandez, O. Eickelberg, D. Hartl, Immune mechanisms in pulmonary fibrosis, Am. J. Respir. Cell Mol. Biol. 55 (3) (2016) 309–322.
[53] Z.-L. Wu, J. Wang, Dioscin attenuates Bleomycin-Induced acute lung injury via inhibiting the inflammatory response in mice, Exp. Lung Res. 45 (8) (2019) 236–244.
[54] M. Liu, X. Zeng, J. Wang, Z. Fu, J. Wang, M. Liu, D. Ren, B. Yu, L. Zheng, X. Hu, W. Shi, J. Xu, Immunomodulation by mesenchymal stem cells in treating human autoimmune disease-associated lung fibrosis, Stem Cell Res. Ther. 7 (63) (2016) 2–15.
[55] E.T. Osei, J.A. Noordhoek, T.L. Hackett, A.I.R. Spanjer, D.S. Postma, W. Timens, C.-A. Brandsma, I.H. Heijink, Interleukin-1 alpha drives the dysfunctional cross-talk of the airway epithelium and lung fibroblasts in COPD, Eur. Respir. J. 48 (2) (2016) 359–369.
[56] M. Gharaee-Kermani, S.H. Phan, Molecular mechanisms of and possible treatment strategies for idiopathic pulmonary fibrosis, Curr. Pharmaceut. Des. 11 (30) (2005) 3943–3971.
[57] Y. Grinberg-Bleyer, D. Saadoun, A. Baeyens, F. Billiard, J.D. Goldstein, S. Gregoire, G.H. Martin, R. Elhage, N. Derian, W. Carpentier, G. Marodon, D. Klatzmann, E. Piaggio, B.L. Salomon, Pathogenic T cells have a paradoxical protective effect in murine autoimmune diabetes by boosting Tregs, J. Clin. Invest. 120 (12) (2010) 4558–4568.
[58] A. Baeyens, D. Saadoun, F. Billiard, A. Rouers, S. Gregoire, B. Zaragoza, Y. Grinberg-Bleyer, G. Marodon, E. Piaggio, B.L. Salomon, Effector T cells boost regulatory T cell expansion by IL-2, TNF, OX40, and plasmacytoid dendritic cells depending on the immune context, J. Immunol. 194 (3) (2015) 999–1010.
[59] J.-H. Zhang, J.-H. Deng, X.-L. Yao, J.-L. Wang, J.-H. Xiao, CD4(+) CD25(+) Tregs as dependent factor in the course of bleomycin-induced pulmonary fibrosis in mice, Exp. Cell Res. 386 (1) (2020) 111700.
[60] K. Chakraborty, S. Chatterjee, A. Bhattacharyya, Impact of Treg on other T cell subsets in progression of fibrosis in experimental lung fibrosis, Tissue Cell 53 (2018) 87–92.